

Forced Precession of a Ferromagnetic Nanoparticle with a Finite Anisotropy Suspended in a Liquid: Nonlinear Aspects

T.V. Lyutyy*, V.V. Reva, N.S. Petrenko, M.O. Pavlyuk

Sumy State University, 2, Rymsky-Korsakov St., 40007 Sumy, Ukraine

(Received 11 September 2019; revised manuscript received 08 October 2019; published online 25 October 2019)

The coupling between mechanical rotation and internal magnetic dynamics of each nanoparticle is an important point of the microscopic description of a ferrofluid interacting with an external field. Here, based on classical equations the deterministic case of the forced coupled precession is described numerically. Our main aim is to study the stable prerecession regimes, which are generated by a rotating external field. In addition to the well-known uniform precession motion, a few nonlinear regimes are observed and discussed. One of them is a nonuniform precession, which was described earlier for the case of an immobilized nanoparticle, where the particle is supposed to be fixed in a solid matrix, and for the case of a rigid dipole, where the nanoparticle magnetization is supposed to be locked in the crystal lattice due to the high anisotropy. Then, the finite anisotropy gives an additional degree of freedom that leads to the generation of the chaotic regime, and one more deterministic regime, which is characterized by oscillations performed synchronously with the external field. A deep understanding of the motion character allows to take control over the heating process in hyperthermia method for cancer treatment. In particular, now it is clear why even a slight tuning of the field frequency can lead to nonlinear growth of the heating rate.

Keywords: Ferrofluid, Ferromagnetic nanoparticle, Finite anisotropy, Coupled motion, Uniform precession, Nonuniform precession, Chaotic dynamics.

DOI: [10.21272/jnep.11\(5\).05021](https://doi.org/10.21272/jnep.11(5).05021)

PACS numbers: 05.45. – a, 47.65.Cb, 75.50.Mm, 82.70. – y

1. INTRODUCTION

A stable interest to ferromagnetic single-domain nanoparticles is arisen from their high potential of applications. The most promising in this regard are biomedical applications such as magnetic particle imaging [1], drug delivery [2], magnetic fluid hyperthermia [3] and cell separation [4, 5]. In this situation, the two issues should be underlined. The first is the development of methods for producing ferromagnetic nanoparticles with specified properties. Up to date, several techniques have already been proposed (see, e.g., [6-8] and references therein). The second is the development of theoretical models aimed at a more complete description of the magnetic properties of ferromagnetic particles in viscous liquids under the action of an alternating magnetic field.

These systems are often studied in the framework of the so-called rigid dipole model, when the particle magnetization is assumed to be fixed along the particle easy axis. This approximation is valid if the anisotropy magnetic field is large enough and allows the use of Newton's second law for rotational motion. Within this model the forced rotation and the influence on it of both thermal fluctuations and dipolar interaction were investigated in [9-11].

However, if the anisotropy magnetic field does not strongly exceed the external field, then the rigid dipole model fails. In this case, we need to take into account the magnetic dynamics inside the rotating framework of the particle body. In the quasi-equilibrium case, when the heat energy is larger than the magnetic one, the description is based on the concept of relaxation times (see, e.g., Ref. [12]). However, the other cases demand the dynamical approach based on equations of motion for the particle and its magnetization that provides a much more complete description of the system properties. Although

these equations were firstly written long time ago, only recently their physical background was stated clearly in [13], and they were applied for studying the coupling between the magnetic and rotational dynamics of a nanoparticle [13-17].

In this paper, we develop the approach used in [17] and pay attention to the features of precession regime of motion induced by a rotating magnetic field. Because of additional degrees of freedom, these regimes can be more complicated in comparison with the cases of a fixed nanoparticle, which are considered in [18]. Thus, in addition to nonuniform and chaotic [19, 20] precession types, some specific regimes are described in detail below.

2. MODEL AND METHODS

We consider a spherical ferromagnetic nanoparticle of radius R , magnetization \mathbf{M} and density ρ . The uniaxial anisotropy is characterized by the anisotropy field H_a . The particle is assumed to be single-domain and the changes in magnetization occur without changing its magnitude ($|\mathbf{M}| = M = \text{const}$), since all the spin magnetic moments always remain parallel due to the strong exchange interaction. Moreover, we suggest that the particle itself can rotate around its center of mass in a liquid with viscosity η .

The motion described above is obeyed the following system of equations in [17]:

$$\dot{\mathbf{n}} = \boldsymbol{\omega} \times \mathbf{n}, \quad (1)$$

$$J\dot{\boldsymbol{\omega}} = \gamma^{-1}V\dot{\mathbf{M}} + V\mathbf{M} \times \mathbf{H} - 6\eta V\boldsymbol{\omega}, \quad (2)$$

$$\dot{\mathbf{M}} = -\gamma(\mathbf{M} \times \mathbf{H}_{\text{eff}}) + \alpha M^{-1} \left[\mathbf{M} \times (\dot{\mathbf{M}} - \boldsymbol{\omega} \times \mathbf{M}) \right], \quad (3)$$

where \mathbf{n} is the unit vector which indicates the direction of the anisotropy axis, $\boldsymbol{\omega}$ is the angular velocity of the

* lyutyy@oeph.sumdu.edu.ua

particle, $J (= 8\pi\rho R^5/15)$ is the moment of inertia, γ is the gyromagnetic ratio, \mathbf{H} is the external uniform field, V is the particle volume, α is the damping parameter, \mathbf{H}_{eff} is the effective magnetic field which takes into account the internal anisotropy field as

$$\mathbf{H}_{\text{eff}} = \mathbf{H} + H_a M^{-1} (\mathbf{M}\mathbf{n}) \mathbf{n}, \quad (4)$$

and, finally, the dot above denotes the time derivative. Further we assume that the particle is under the action of the external circularly polarized homogeneous field

$$\mathbf{H} = \mathbf{e}_x H \cos \Omega t + \mathbf{e}_y H \sigma \sin \Omega t, \quad (5)$$

where $\mathbf{e}_x, \mathbf{e}_y$ are the unit vectors of the Cartesian coordinate system, H and Ω are the field amplitude and frequency, respectively, t is the time, and $\sigma (= \pm 1)$ is the factor determining the field polarization direction.

In the case when the inertia term in (2) is negligible, this equation can be transformed into a more convenient form. Then, we transform the equation for the internal magnetic dynamics (3) in order to separate the terms containing the time derivatives. As a result, we obtain

$$\dot{\mathbf{n}}\Omega_{\text{cr}}^{-1} = \dot{\mathbf{m}} \times \mathbf{n}\Omega_{\text{r}}^{-1} + (\mathbf{m} \times \mathbf{h}) \times \mathbf{n}, \quad (6)$$

$$(1 + \alpha_1^2)\Omega_{\text{r}}^{-1}\dot{\mathbf{m}} = -\mathbf{m} \times \mathbf{h}_{\text{eff}}^1 - \alpha_1 \mathbf{m} \times \mathbf{m} \times \mathbf{h}_{\text{eff}}^1, \quad (7)$$

where $\beta = \alpha M/6\gamma\eta$, $\Omega_{\text{r}} = \Omega/(1 + \beta)$, $\alpha_1 = \alpha/(1 + \beta)$, $\mathbf{m} = \mathbf{M}/M$, $\mathbf{h} = \mathbf{H}(t)/H_a$ and

$$\mathbf{h}_{\text{eff}}^1 = (\mathbf{e}_x h \cos \Omega t + \mathbf{e}_y h \sigma \sin \Omega t)(1 + \beta) + (\mathbf{m}\mathbf{n}) \mathbf{n}. \quad (8)$$

To further numerical studies, one can transform the equations of motion into the scalar form with respect to the spherical coordinates of vectors \mathbf{m} and \mathbf{n} as follows from

$$\mathbf{m} = (\sin \vartheta \cos \varphi, \sin \vartheta \sin \varphi, \cos \vartheta),$$

$$\mathbf{n} = (\sin \theta \cos \phi, \sin \theta \sin \phi, \cos \theta).$$

After standard transformations and accounting (5), we can write

$$(1 + \alpha_1^2)\Omega_{\text{r}}^{-1}\dot{\vartheta} = f_1 + \alpha_1 f_2, \quad (9)$$

$$(1 + \alpha_1^2)\Omega_{\text{r}}^{-1}\dot{\varphi} = \csc \vartheta (\alpha_1 f_1 - f_2), \quad (10)$$

$$\Omega_{\text{r}}^{-1}\dot{\theta} = \beta\alpha^{-1} [\omega_y \cos \phi - \omega_x \sin \phi], \quad (11)$$

$$\Omega_{\text{r}}^{-1}\dot{\phi} = \beta\alpha^{-1} [\omega_z - \cot \theta (\omega_y \sin \phi + \omega_x \cos \phi)], \quad (12)$$

$$f_1 = h(1 + \beta) \sin(\sigma\Omega t - \varphi) - F \sin \theta \sin(\varphi - \phi), \quad (13)$$

$$f_2 = \cos \vartheta [h(1 + \beta) \cos(\sigma\Omega t - \varphi) + F \sin \theta \cos(\varphi - \phi)] - F \sin \vartheta \cos \theta, \quad (14)$$

$$F = \cos \theta \cos \vartheta + \cos(\varphi - \phi) \sin \theta \sin \vartheta (= \mathbf{m}\mathbf{n}), \quad (15)$$

$$\omega_x = \Omega_{\text{r}}^{-1} (\dot{\vartheta} \cos \vartheta \cos \varphi - \dot{\varphi} \sin \vartheta \sin \varphi) - (1 + \beta) h \sin \vartheta \sin \sigma\Omega t, \quad (16)$$

$$\omega_y = \Omega_{\text{r}}^{-1} (\dot{\vartheta} \cos \vartheta \sin \varphi + \dot{\varphi} \sin \vartheta \cos \varphi) + (1 + \beta) h \cos \vartheta \cos \sigma\Omega t, \quad (17)$$

$$\omega_z = (1 + \beta) h \sin(\sigma\Omega t - \varphi) \sin \vartheta - \Omega_{\text{r}}^{-1} \dot{\theta} \sin \vartheta. \quad (18)$$

The system of four equations (9)-(12) with designations (13)-(16) has been solved using the 4th order Runge-Kutta method for the system parameters $\alpha = 0.1$, $M = 228$ G, $\eta = 0.006$ and the following parameters of simulation: time step was chosen as 10^{-3} of the field period. The stable solutions were seeking by the comparison of the trajectories on every 10^4 field periods, while the stable solution was not found, or the maximum simulation time of 10^7 field periods was not reached. The precession criterion was chosen as 10^{-5} . The initial conditions were chosen as $\vartheta = \vartheta_{\text{in}} = 0.005$, $\theta = \theta_{\text{in}} = 0.0051$, $\varphi = \varphi_{\text{in}} = 0.005$, $\phi = \phi_{\text{in}} = 3.14$.

Finally, in our calculation we used the reduced frequency $\tilde{\Omega} = \Omega/\Omega_{\text{r}}$ to our convenience.

3. RESULTS AND DISCUSSION

The simplest case is the uniform precession regime. For the case of coupled mechanical and magnetic rotation it was described in [15, 16]. In a brief this regime consists in precession of vectors \mathbf{m} and \mathbf{n} with external field \mathbf{h} in synchronous way. It is describing in full by four angle constants as $\vartheta = \vartheta_0$, $\theta = \theta_0$, $\varphi = \varphi_0$, $\phi = \phi_0$. Here the first pair determines the precession cones, while the second one – the lags between vectors \mathbf{m} and \mathbf{n} and field \mathbf{h} . It is important that cone for \mathbf{n} is always narrower than cone for \mathbf{m} .

Both the precession and the lag angles grow with frequency and amplitude, and the uniform precession can become unstable. The magnetic moment \mathbf{m} tries to catch vector \mathbf{h} and in addition to the precession is being involved in oscillations similar to the so-called nutation. These oscillations have large enough amplitude and their frequency is not a multiple of the field one. Therefore, the oscillations occur asynchronously with the field. For the case of a fixed nanoparticle, the same behavior was observed in [18]. In the present case, the easy axis is not fixed rigidly and it is involved in such oscillations with a few peculiarities. First, for realistic system parameters, the oscillation amplitude of the easy axis and its average value are much smaller than those for \mathbf{m} .

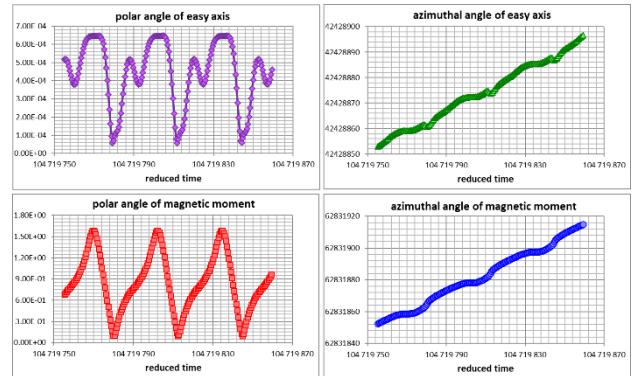


Fig. 1 – Time evolutions of angular coordinates of the nanoparticle driven by the rotating field (5) of reduced amplitude $h = 0.14$ and reduced frequency $\tilde{\Omega} = 0.6$. The rotating frequencies for magnetic moment and easy axis are different and not a multiple of the field period

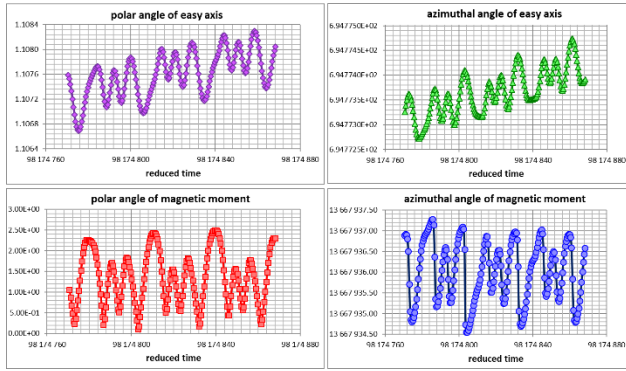


Fig. 2 – Time evolutions of angular coordinates of the nanoparticle driven by the rotating field (5) of reduced amplitude $h = 0.14$ and reduced frequency $\tilde{\Omega} = 0.64$. This regime is pure chaotic because of slow chaotic drift of the averaged position of the magnetic moment and easy axis and irregular oscillations around them

Second, as it can be seen from scales of axes in Fig. 1, the rotating frequency of \mathbf{n} is smaller than for \mathbf{m} . The different rotating frequencies in nonuniform regime are an interesting result, since for uniform precession this is not observed.

With further increasing frequency, the average position of the vector \mathbf{n} demonstrates a drift, which can be performed in different ways. Naturally that due to the anisotropy, vector \mathbf{m} is also involved in the drift. The first drift scenario is pure chaotic, when both the average position and oscillations around it are irregular. At that, the drift is much slower than the oscillations. This regime is depicted in Fig. 2. Here the violation of the deterministic character of the plot is especially pronounced for time evolution of the magnetic moment azimuthal angle. Such chaotic picture was reported in [19, 20] for the case of the magnetic dynamics of a fixed nanoparticle driven by a linearly polarized field.

For larger frequencies, the transformation of the motion type occurs. Here, the trends of vectors \mathbf{m} and \mathbf{n} remain chaotic, but the oscillations become regular and their frequencies coincide with the field one, see Fig. 3. Scale of plots does not let to see that the drift of the average position of vectors \mathbf{m} and \mathbf{n} is performed in a wide range of coordinates, but one can calculate that these average positions are very close to each other.

The next regime is regular, although keeps some properties of the previous two modes. Here, a slow drift takes place only by the azimuthal angles of vectors \mathbf{m} and \mathbf{n} , while the polar angles demonstrate the oscillations only. The drift of the vector \mathbf{n} is clearly seen in Fig. 4, while the drift of \mathbf{m} is not in the plot scale. Nevertheless, it exists because of anisotropy coupling. This regime is typical around the resonance frequency. In the case of the parameters chosen, for the field amplitude of 0.14 it is realized in the reduced frequency range 0.77-0.96. The dependencies of angular trajectories on the initial conditions and the time step value were not observed. It allows us to state that this regime is regular.

The character of the last regimes is connected to the reorientations of the vectors \mathbf{m} and \mathbf{n} under the action of the rotating field. Despite the initial conditions for polar angles are chosen close to zero, the stable regimes are realized only in a vicinity of π . Naturally that the uniform

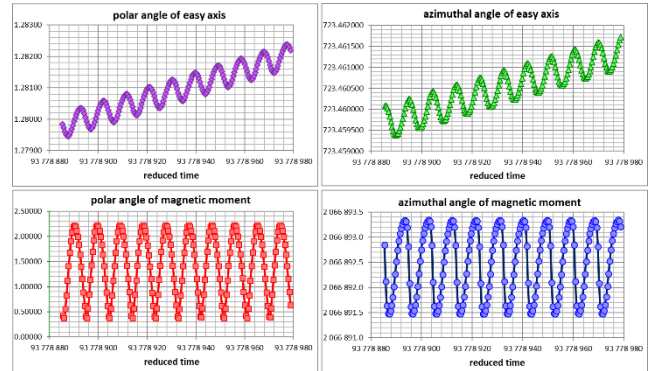


Fig. 3 – Time evolutions of angular coordinates of the nanoparticle driven by the rotating field (5) of reduced amplitude $h = 0.14$ and reduced frequency $\tilde{\Omega} = 0.67$. This regime is chaotic because of slow chaotic drift of the averaged position of the magnetic moment and easy axis

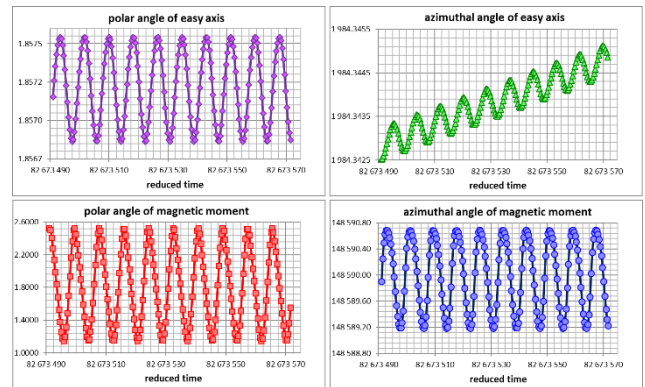


Fig. 4 – Time evolutions of angular coordinates of the nanoparticle driven by the rotating field (5) of reduced amplitude $h = 0.14$ and reduced frequency $\tilde{\Omega} = 0.76$. This regime is regular. The slow drift of the averaged position of the magnetic moment and easy axis occurs through the changes of azimuthal angles only

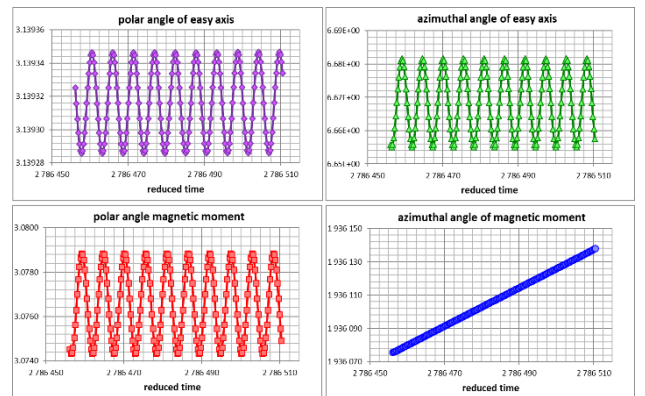


Fig. 5 – Time evolutions of angular coordinates of the nanoparticle driven by the rotating field (5) of reduced amplitude $h = 0.14$ and reduced frequency $\tilde{\Omega} = 1.15$. The magnetic moment performs the uniform precession, while the easy axis sticks in oscillations. It can be a prolonged transition process

precession here is the stable solution. However, due to the narrow precession cones, the easy axis can avoid the rotation and performs the only oscillations instead, see Fig. 5. It seems that this regime is a very long transition process, but even in this case from practical point of view it is reasonable to treat such situation as a separate regime.

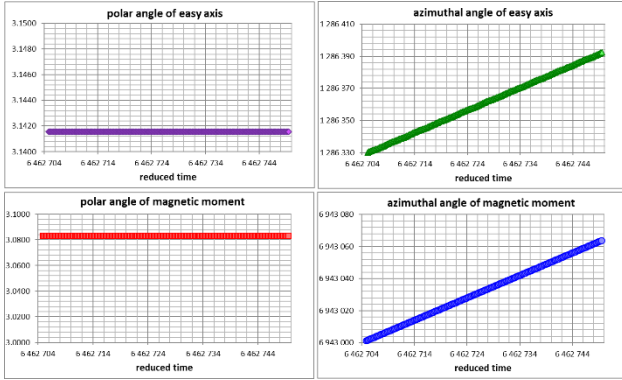


Fig. 6 – Time evolutions of angular coordinates of the nanoparticle driven by the rotating field (5) of reduced amplitude $h = 0.14$ and reduced frequency $\tilde{\Omega} = 1.45$. The uniform precession in the “down” state is generated

Finally, the pure uniform mode can be achieved faster for a larger frequency (Fig. 6). We note that in comparison with the previous case, here the residual oscillations are one order smaller. It confirms the validity of the assumption about existing additional nonlinear regime before the linear one.

Finally, the last observed example of the nonlinear behavior is the so-called intermediate or secondary uniform regime (Fig. 7). It is generated because of the stability reconstruction. Strictly speaking, all the nonlinear types of motion occur when the uniform precession does not satisfy the stability criteria in some ranges of the field frequency and amplitude. And ranges where the uniform precession is stable can alternate with the nonstable ranges. This effect is well known, and it was described in [18] for the fixed particle case. The transition to the secondary uniform precession mode occurs abruptly with the smallest change of the field parameters near the transition point. In our case, for the parameters chosen, the transition point is near the values $h = 0.14$ and $\tilde{\Omega} = 0.63$, but here the secondary uniform precession borders with the nonuniform and chaotic regimes. However, one can assume that the transition to the secondary uniform mode from the common one is possible. In this case, the transition will be accompanied by the jumps of precession angles.

4. CONCLUSIONS

The numerical analysis of the coupled magnetic dynamics and mechanical rotation of the uniaxial nanoparticle in a viscous liquid under the action of the rotating magnetic field was performed. Within this, we based on the classical deterministic equations [13] that account correctly the peculiarities of the motion. The data obtained for the realistic system parameters was analyzed. It allows us to conclude the following.

The existence of the uniform rotation regime predicted analytically was confirmed by simulations. The main feature of this motion is the small precession cone

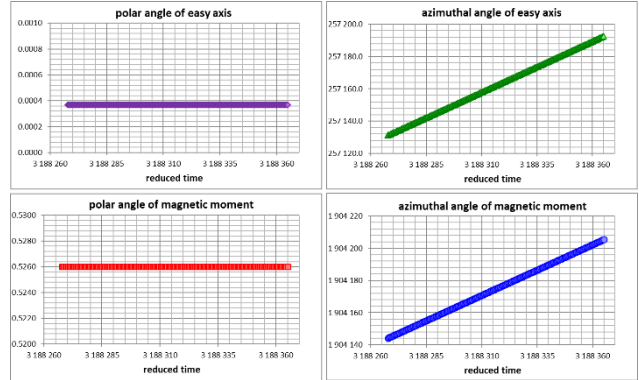


Fig. 7 – Time evolutions of angular coordinates of the nanoparticle driven by the rotating field (5) of reduced amplitude $h = 0.14$ and reduced frequency $\tilde{\Omega} = 0.63$. The intermediate or secondary uniform precession is generated. The precession cone of easy axis is much narrower

angle for easy axis that assumes a weak mechanical rotation of the nanoparticle body. Also, the so-called up and down types of the uniform precession caused by the uniaxial anisotropy were observed. It is important for understanding the hysteresis properties of ferrofluids.

Then, we report the existence of the nonuniform precession regime when both the magnetic moment of the nanoparticle and its easy axis (represented by vectors \mathbf{m} and \mathbf{n} , respectively) perform regular oscillations of a period, which is not a multiple of the field one. This regime is observed in the case of a rigidly fixed nanoparticle and a rigid dipole cases. However, the oscillation patterns of \mathbf{m} and \mathbf{n} here are different.

Finally, we have observed at least two new regimes, which do not exist for a rigidly fixed nanoparticle and a rigid dipole cases under the action of the circularly polarized field. The first new mode is the chaotic precession which is realized in two different ways: pure chaotic (Fig. 2) and slow chaotic drift of \mathbf{n} with “regular” oscillations of \mathbf{m} around \mathbf{n} (Fig. 3). The second new mode is regular where a slow drift is realized by the azimuthal angles of the vectors \mathbf{m} and \mathbf{n} , while the polar angles of these vectors oscillate around constant means.

The relevance of these studies is closely connected to the control of the power losses and heating processes during the magnetic hyperthermia therapy. In particular, the different precession regimes lead to different power losses, and switching between them causes the abrupt changes of the heating intensity. The latter can be used or must be prevented, but in any cases, it should be well studied.

ACKNOWLEDGEMENTS

This work was partially supported by Germany-Ukraine bilateral cooperation Project DFG (HA 1517/42-1) – DFFD (Φ -81=41894). In addition, the authors acknowledge the support of the Ministry of Education and Science of Ukraine under Grant No 0119U100772.

REFERENCES

1. Q.A. Pankhurst, J. Connolly, S.K. Jones, J. Dobson, *J. Phys. D: Appl. Phys.* **36** No 13, R167 (2003).
2. K. Ulbrich, K. Hola, V. Šubr, A. Bakandritsos, J. Tuček, R. Zbořil, *Chem. Rev.* **116**, 5338 (2016).
3. E.A. Périgo, G. Hemery, O. Sandre, D. Ortega, E. Garaio, F. Plazaola, F.J. Teran, *Appl. Phys. Rev.* **2**, 041302 (2015).
4. M. Hejazian, W. Li, N.T. Nguyen, *Lab Chip* **15**, 959 (2015).
5. A. Dalili, E. Samiei, M. Hoorfar, *Analyst* **87**, 144 (2019).
6. R. Hao, R. Xing, Zh. Xu, Ya. Hou, S. Gao, Sh. Sun, *Adv. Mater.* **22**, 2729 (2010).
7. O.V. Yelenich, S.O. Solopan, T.V. Kolodiazhnyi, V.V. Dzyublyuk, A.I. Tovstolytkin, A.G. Belous, *Mater. Chem. Phys.* **149**, 129 (2014).
8. K. Zhu, Ya. Ju, J. Xu, Z. Yang, S. Gao, Ya. Hou, *Acc. Chem. Res.* **51**, 404 (2018).
9. B.U. Felderhof, R.B. Jones, *J. Phys.: Condens. Matter* **15**, 4011 (2003).
10. Y.L. Raikher and V.I. Stepanov, *Phys. Rev. E* **83**, 021401 (2011).
11. Zh. Zhao, C. Rinaldi, *J. Phys. Chem. C* **122**, 21018 (2018).
12. R.E. Rosensweig, *J. Magn. Magn. Mater.* **252**, 370 (2002).
13. K.D. Usadel, C. Usadel, *J. Appl. Phys.* **118**, 234303 (2015).
14. H. Keshtgar, S. Streib, A. Kamra, Ya.M. Blanter, G.E.W. Bauer, *Phys. Rev. B* **95**, 134447 (2017).
15. T.V. Lyutyi, O.M. Hryshko, A.A. Kovner, E.S. Denisova, *J. Nano. Electron. Phys.* **8**, 04086 (2016).
16. T.V. Lyutyi, O.M. Hryshko, A.A. Kovner, *J. Magn. Magn. Mater.* **446**, 87 (2018).
17. T.V. Lyutyi, O.M. Hryshko, M.Y. Yakovenko, *J. Magn. Magn. Mater.* **473**, 198 (2019).
18. S.I. Denisov, T.V. Lyutyi, C. Binns, P. Hänggi, *J. Magn. Magn. Mater.* **322**, 1360 (2010).
19. D.V. Vagin and O.P. Polyakov, *J. Appl. Phys.* **105**, 033914 (2009).
20. J. Bragard, H. Pleiner, O.J. Suarez, P. Vargas, J.A.C. Gallas, D. Laroze, *Phys. Rev. E* **84**, 037202 (2011).

Вимушена прецесія ферромагнітної наночастинки зі скінченною анізотропією, зваженої в рідині: нелінійні аспекти

Т.В. Лютий, В.В. Рева, Н.С. Петренко, М.О. Павлюк

Сумський державний університет, вул. Римського-Корсакова, 2, 40007 Суми, Україна

Зв'язок між механічним обертанням та внутрішньою магнітною динамікою наночастинки є важливим аспектом мікроскопічного опису поведінки фероріднини, що взаємодіє із зовнішнім полем. В нашій роботі на основі класичних рівнянь чисельно описаний детермінований випадок вимушеної сумісної прецесії. Основною метою роботи є вичерпний опис усталених режимів прецесії, які генеруються обертовим зовнішнім полем. Крім відомої однорідної прецесії, було виявлено та описано кілька нелінійних режимів. Один з них – це неоднорідна прецесія, яка була описана раніше для випадку знерухомленої наночастинки, коли частинка розглядалась як закріплена у твердій матриці, і для випадку жорсткого диполя, коли намагніченість наночастинки розглядалась як зафіксована в кристалічній решітці завдяки великій анізотропії. Скінченна анізотропія дає додаткову ступінь свободи, що призводить до виникнення хаотичного режиму та ще одного детермінованого режиму, для якого характерні коливання, що виконуються синхронно із зовнішнім полем. Глибоке розуміння характеру руху дозволяє контролювати процес нагріву під час гіпертермії – метод терапії ракових пухлин. Зокрема, тепер зрозуміло чому навіть незначна підстройка частоти поля може призвести до нелінійного зростання швидкості нагріву.

Ключові слова: Ферорідина, Ферромагнітна наночастинка, Скінченна анізотропія, Зв'язаний рух, Однорідна прецесія, Неоднорідна прецесія, Хаотична динаміка.